

## Modeling Vehicle Flocking in Lane-Free Automated Traffic

Majid Rostami-Shahrbabaki<sup>1</sup> , Simone Weikl<sup>1</sup> , Tanja Niels<sup>1</sup> ,  
and Klaus Bogenberger<sup>1</sup> 

Transportation Research Record  
1–14

© National Academy of Sciences:  
Transportation Research Board 2023



Article reuse guidelines:

[sagepub.com/journals-permissions](https://sagepub.com/journals-permissions)

DOI: 10.1177/03611981231159405

[journals.sagepub.com/home/trr](https://journals.sagepub.com/home/trr)



### Abstract

In automated lane-free traffic, vehicles can choose any arbitrary lateral location. This enables vehicle flocking where, compared to platooning, the grouping of vehicles is possible with smaller space gaps, not only longitudinally but also laterally. Vehicle flocking can fulfill several purposes, such as increasing the road capacity, saving energy by reducing the aerodynamic drag force, and dampening shockwaves. Within this paper, we develop a control framework for modeling vehicle flocks in automated lane-free traffic. The proposed control algorithm considers two types of agents:  $\alpha$ -agents representing potential flock mates and a  $\gamma$ -agent representing the virtual leader with collective objectives (e.g., slowing down in the case of traffic congestion ahead). Our algorithm is based on energy functions for flock centering and collision avoidance, a consensus algorithm for velocity matching, and navigational feedback exerted by the virtual leader. The virtual leader's path, which should be followed by the flock, is defined in an upper-level controller. In addition, a feedback algorithm for dynamic road boundary control is implemented. We simulate the proposed approach with very promising results. We show that vehicle flocks are efficiently formed within a few seconds, speeds are successfully aligned, and vehicle arrangements stay stable under different scenarios. In addition, the lateral and longitudinal flock extension changes with different energy functions and changing road boundaries, and vehicle flocks follow the trajectory of the virtual leader. Most importantly, vehicle flocks stay stable in the case of perturbations and the induced shock is dampened efficiently because of slight changes in the vehicles' lateral locations.

### Keywords

operations, advanced technology, algorithm, automated/autonomous vehicles, connected vehicles, simulation

The transportation sector in the 21st century faces enormous challenges. The rise in vehicle miles traveled on limited, costly transportation infrastructure leads to massive traffic congestion, causing environmental and economic damages and reduced traffic safety. The emergence and advancement of connected and automated vehicles (CAVs) equipped with highly precise sensors and smart technologies for fast and reliable vehicle-to-vehicle (V2V) and vehicle-to-infrastructure (V2I) communication offers the possibility to develop new road management strategies. CAVs are able to make fast decisions based on control strategies to avoid collisions, efficiently move forward, and also cooperate with other vehicles. In freeway traffic, for example, CAV platoons can be formed that drive with a very short headway, resulting in fuel saving and increased highway capacity (1). While the platoon speeds of human-driven vehicles will depend on the

speed of the front vehicle, CAV platoons can agree on a common desired speed or follow external recommendations (2). If receiving further information, platoons can optimally plan their trajectories, for example, to smoothly decelerate when downstream congestion is detected (3) or to minimize fuel consumption based on a given road inclination (2). However, the benefits only apply to the vehicles in one specific lane and long platoons can hinder other vehicles from performing lane changes or even entering or leaving the freeway (4). Considering that CAVs cannot only cooperate with

<sup>1</sup>Chair of Traffic Engineering and Control, Technical University of Munich, Munich, Germany

### Corresponding Author:

Majid Rostami-Shahrbabaki, [majid.rostami@tum.de](mailto:majid.rostami@tum.de)

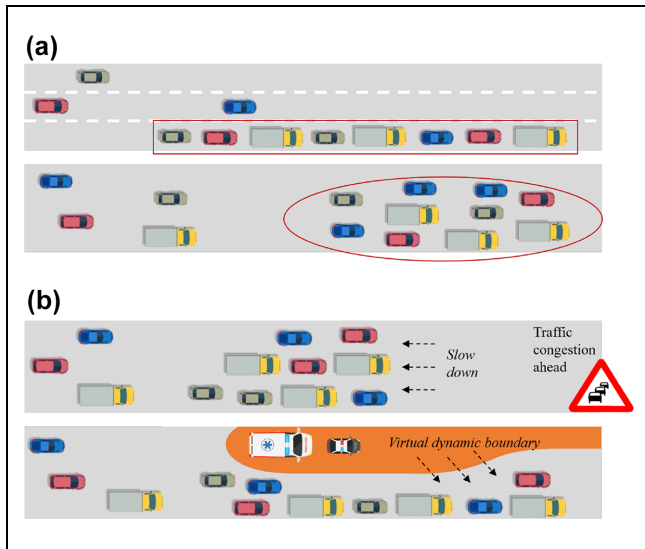


**Figure 1.** Examples of vehicular flocking: (a) schematic representation of a vehicle platoon and a vehicle flock and (b) flock management use cases.

vehicles in front or behind them but also with all surrounding vehicles, lane changes can be performed cooperatively and, eventually, the sheer need for fixed vehicle lanes can be questioned in the case of a fully connected and automated environment. Vehicle lanes were introduced as essential instruments for simplifying driving tasks for human drivers and increasing traffic safety when automobiles prevailed as an important means of transport with higher speeds in the 20th century. However, as stated by Papageorgiou et al. (5), this happened at the expense of road capacity, as lanes reduce the lateral static occupancy on motorways by almost 50%. Additional dynamic capacity loss is caused by lane-changing maneuvers. Papageorgiou et al. (5) introduced a novel paradigm for freeway traffic in which vehicles are not limited to traffic lanes but rather can use the entire road width, allowing for an increase in the efficiency of traffic operations. Recent evaluations demonstrate a great potential for increasing road capacity in a fully automated lane-free environment (6). The positive impacts could further be increased by traffic management strategies that support the formation of groups of vehicles with certain headways and speeds.

Since lanes no longer exist in the assumed lane-free traffic environment, flocking will be developed as a generalization of platooning. Flocking is considered a novel approach for grouping vehicles not only longitudinally, but also laterally (Figure 1a shows an example). It is inspired by flocking phenomena observed in nature (e.g., from birds and fish) and can fulfill several purposes, such as increasing the road capacity, saving energy by reducing the drag force, sharing resources (e.g., electric

charging, internet), and playing the role of a traffic control measure. This paper builds on previous publications by Berahman et al. (6) and Rostami-Shahrababaki et al. (7) and extends the existing concepts by introducing a new flock management layer that allows for achieving certain vehicle headways, flock speeds, and lateral distributions of vehicles on the road. Potential use cases of such a flock management are shown in Figure 1b. They include variable speed limits in oversaturated traffic conditions, optimally navigating vehicles through curves or construction zones, or making a flock move to the side to let an emergency vehicle pass.

The outline of the paper is as follows: the next section provides the background and most relevant literature with respect to vehicular flocks. Following that, the applied methodology is explained in detail. The simulation setup that is used for the implementation and evaluation of the presented concept is described afterward. The section following that discusses the results and shows the key features of the algorithm. Finally, a conclusion and outlook are given in the conclusion section.

## Background and Literature Review

### CAV Platoons

CAV platoons take advantage of fast and reliable V2V communication and automated maneuvering to significantly reduce vehicle headways. Several papers present algorithms for platoon formation and analyze their effects on individual fuel consumption as well as overall environmental, traffic safety, and capacity benefits (8–11). Smaller vehicle gaps are beneficial with respect to the aerodynamic drag force and can therefore significantly reduce fuel or energy consumption (9, 10). In addition, freeway capacity is increased if vehicles are able to drive at shorter distances (8). One important requirement for platooning algorithms is string stability, that is, ensuring that small disturbances with the front vehicle's trajectory are not amplified along the vehicle string (12, 13). Platoon forming can be challenging if vehicles in the platoon have different destinations (14).

### CAV Platoons Across Multiple Lanes

Motivated by the goal of further increasing road capacity, a few researchers have developed concepts for lane-based platooning across multiple lanes. Kato et al. (15) conducted a simulation study on cooperative driving formations across multiple lanes with vehicles starting from an initial state. Their model could handle different events, such as splitting, merging, overtaking, and obstacle avoidance. Several researchers (16–20) used ideas from swarm robotics for developing multiple-lane platooning strategies that control each vehicle in the group

longitudinally and laterally. Hao et al. (21) developed a model that manages platoons in two dimensions at signalized intersections. Xu et al. (22) proposed a method for multi-lane vehicle formation control that is combined with a method to calculate conflict-free passing sequences at unsignalized intersections.

### Lane-Free CAV Traffic

According to Papageorgiou et al. (5), the lateral occupancy in current lane-based traffic on motorways is only slightly higher than 50% and additional capacity losses are caused by lane-changing maneuvers. Motivated by this fact, they introduced the novel paradigm of lane-free vehicular traffic for CAVs: the so-called TrafficFluid concept. It is based on the assumption that in the not-too-far future CAVs can communicate with each other (V2V) and with the infrastructure (V2I) precisely, quickly, and reliably, making the need for traffic lanes as structuring elements obsolete. The TrafficFluid concept is based on two combined principles: “lane-free traffic” and “nudging.” Within lane-free traffic, vehicles are not limited to traffic lanes but rather can use the entire road width and choose any arbitrary lateral location, allowing for an increase in the efficiency of traffic operations. Nudging describes the effect of vehicles in front changing their behavior as they sense the presence of other vehicles with a higher desired speed, basically quitting the anisotropy of traffic flow resulting from human drivers.

In Sekeran et al. (23), an overview of the history of lane-free traffic is provided. Malekzadeh et al. (24, 25) extended the TrafficFluid concept by mathematical models for real-time internal boundary control by which the total road width is shared among the two directions in dependence of the bi-directional demand. Thereby, the total flow efficiency of both directions can be maximized. Control strategies and path planning algorithms for CAVs in the lane-free environment were designed by Levy and Haddad (26), Karafyllis et al. (27), Yanumula et al. (28), and Troullinos et al. (29). These strategies avoid collisions with other vehicles, obstacles, and the road boundary and optimize vehicle speeds. Some of them also cover additional objectives, such as minimizing fuel consumption or maximizing passenger comfort. Most approaches are based on longitudinal and lateral artificial forces/potential fields that determine the two-dimensional vehicle acceleration. Troullinos et al. (30) developed a simulator (TrafficFluid-Sim) for CAVs in lane-free traffic built on the open-source traffic simulation software SUMO. Using this simulator, in Rostami-Shahrabaki et al. (31), a so-called potential line approach is developed by which each vehicle receives a specific desired lateral location based on its desired speed. This approach mimics the behavior of today’s

traffic where faster vehicles drive on the right-hand side of the road, which leads to much higher throughput because of the harmonized traffic movements. Berahman et al. (6) proposed a driving strategy for CAVs in the lane-free traffic environment combining artificial forces and a reinforcement learning approach. An artificial ellipsoid border is assumed around each vehicle with lateral and longitudinal forces to reach closer space gaps, supplemented by an additional longitudinal repulsive force for avoiding longitudinal collisions. The methodology was implemented in the SUMO traffic simulator and promising results were shown: the maximum traffic flow in the lane-free scenarios was about two times higher than in lane-based traffic and the speed deviation from the vehicles’ desired speeds at maximum flow was around half that of the lane-based model. This shows the great potential of lane-free traffic for increasing road capacity.

### The Concept of Flocking

According to Caruntu et al. (19), flocking is a simple approach in which entities form large groups without colliding, based on local interactions, to move toward a common target. The flocking phenomenon can be observed in nature, where some natural species, such as birds, fish, or ants, travel as a flock, school, or herd for various reasons: to protect themselves from the threat of predators; to search for food; for energy efficiency; or for social and mating activities. There is no central control unit. The complex but coordinated flock formation and motion are merely the aggregate result of the actions of individuals based on their local perception. In comparison to structured approaches where individuals follow a leader with a fixed path, this is a self-organized behavioral approach with decentralized control in which each individual has a desired behavior. According to Reynolds (32), flock behavior is produced by three basic, simple rules of interaction:

1. flock centering: individuals should stay close to other individuals in the flock;
2. collision avoidance: collisions with other flock members have to be avoided;
3. velocity matching: individuals should travel at a common speed.

Flocking was analyzed by numerous studies for animals (33, 34) and chemical entities (35), and adapted to mobile robots (36, 37), autonomous drones (38), satellites (39), general multi-agent systems (40, 41) and more. There are several reasons for the application of flocking within these use cases: using space more efficiently, reducing space gaps for resource sharing, or saving energy in operations.

Most control strategies for flock formations are based on artificial forces, consensus control, and graph theory. The Reynolds rules can be modeled by potential fields based on artificial forces. Attractive forces make individuals join formations, while repulsive forces make them avoid collisions with obstacles and flock mates. The individuals move along the gradient direction of the potential fields. Within consensus control approaches, individuals use the aggregate information from neighbors to reach a common goal, for example, the weighted average of speeds. Within graph theoretical approaches, vertices represent individuals and edges indicate the communication between these. Based on these approaches, specific formations among vehicles can be reached.

### CAV Flocking in Lane-Free Traffic

The general road capacity increase within lane-free traffic could be further amplified by the application of CAV flocking. Compared to platoons in lane-based traffic, CAV flocks have more degrees of freedom for choosing positions and thus can reach significantly smaller lateral and longitudinal space gaps. Besides that, CAV flocks could fulfill additional purposes: saving energy by building aerodynamically efficient formations and reducing the drag force, sharing resources (e.g., electric charging, internet) among CAVs in a flock or playing the role of a traffic control measure (e.g., dampening speeds). However, until now few studies have dealt with vehicular flocking in non-lane-discipline or lane-free traffic. Tang and Li (42) developed stable longitudinal and lateral consensus-based control protocols for flocking of non-lane-discipline CAVs. Chuang et al. (43) developed cooperative control algorithms for CAV flocking using pairwise attractive–repulsive interactions. The authors found that critical thresholds exist between coherent, stable, and scalable flocking and the dispersed or collapsing motion of the group. Rostami-Shahrbabaki et al. (7) developed a decentralized two-layer approach for vehicular flocking in lane-free traffic. In the tactical layer, the control mode is defined and vehicles are matched. In the operational layer, the inter-vehicle forces and vehicle movements are calculated based on defined motion dynamics. Self-organized, collision-free vehicular flocks result from the defined flock attraction and repulsion forces.

Compared to the authors' previous work (7), which considered different zones and control modes for the movement of vehicles, in this work, vehicular flocking is developed using a single energy function and the principles of graph theory. The general framework is built on the flocking algorithm developed by Olfati-Saber (41). A dynamic graph is constructed based on the elliptic distance between the vehicles in the flock. This graph is

used in the consensus approach for velocity matching of the flock members. The developed energy function provides the necessary inter-vehicle force for flock repulsion and attraction. Based on this function, the vehicles are automatically located in the flock, where the total energy is minimized, unless there are some constraints, such as boundary conditions, that result in vehicle locations where the energy level is higher. In addition, the control algorithm considers the behavior of a virtual leader as the navigational feedback for the adaptation of the flock to a desired path and speed. The developed methodology is explained in detail in the following section.

## Methodology

Each vehicle is modeled using discrete double integrator dynamics and moves on the road with implied longitudinal and lateral accelerations. The discrete-time setup is best suited to the computer implementation of the approach. The control algorithm has three terms: (1) flocking force, (2) consensus term, and (3) navigational feedback derived from the virtual leader. The overall methodology is visualized in Figure 2. The top part of the figure shows that the flocking force (part 1) is realized via an energy function that applies to each individual vehicle in the flock (denoted as the  $\alpha$ -agent) and depends on the distances and relative positions to its neighbors. The consensus term (part 2) ensures that vehicles within the flock drive at similar speeds. To implement the consensus algorithm, the topology of the flock is modeled as a spatial graph and a weighted adjacency matrix is derived. The navigational feedback (part 3) is realized via a virtual leader (denoted as the  $\gamma$ -agent) with a given trajectory that guides the flock in case of traffic congestion or curves. The virtual leader could be any vehicle of the flock or an external control unit. In addition, vehicle accelerations are bound because of the physical limitations of the vehicles and the road boundary.

In the following sections, the vehicle dynamics are first described, followed by the graph definition. The details of the control algorithm (along with the description of the bottom part of Figure 2) are given afterwards.

### Basic Definitions

**Vehicle Dynamics.** In the lane-free environment, the lateral and longitudinal positions of the vehicle on a two-dimensional plane are considered as the vehicle output. As input commands, the vehicle is controlled by the respective accelerations in the longitudinal and lateral directions. The motion dynamics for a given vehicle  $i$  are described with the following discrete-time equations in the longitudinal and lateral directions:

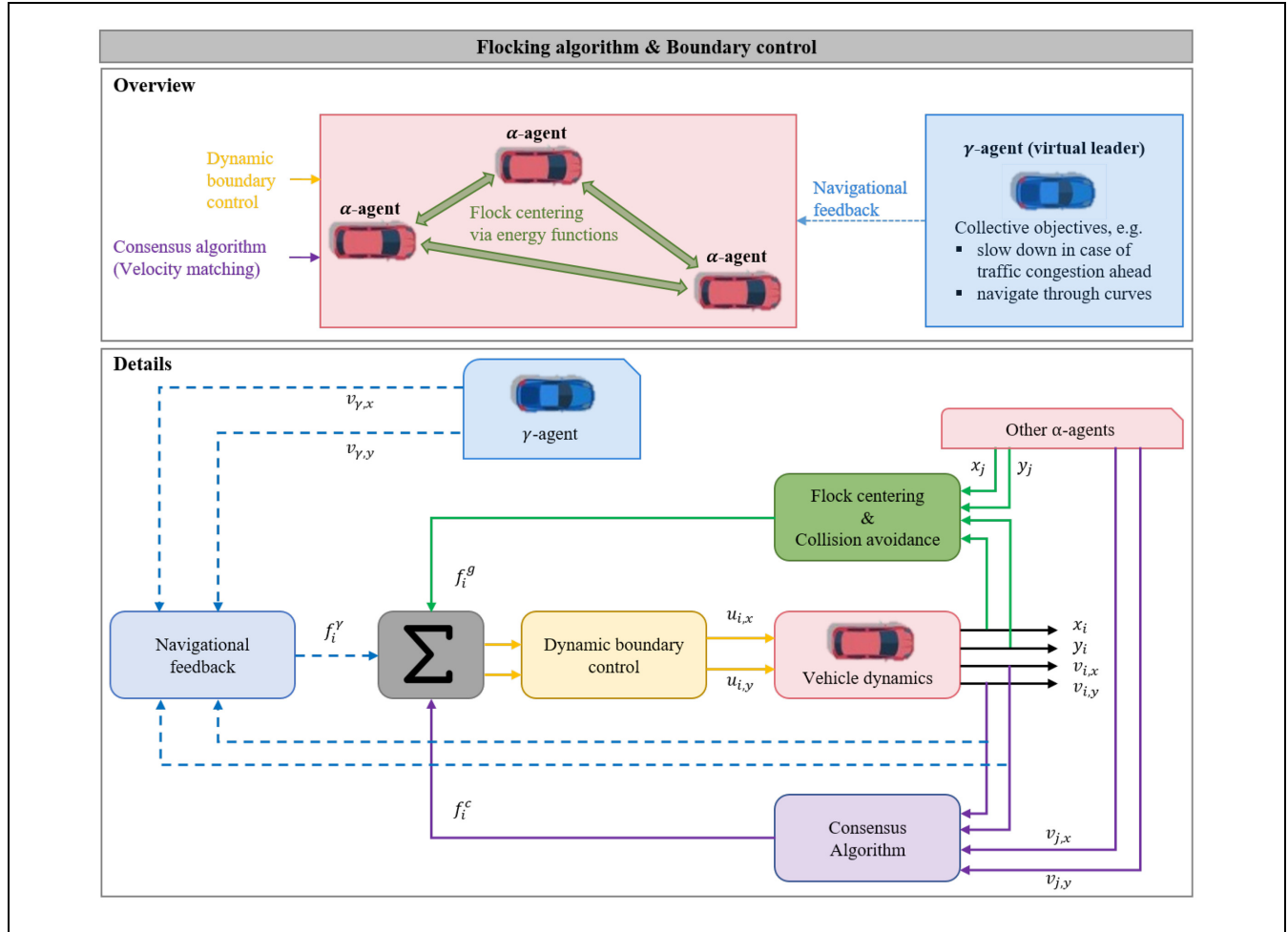


**Figure 2.** Overview of the methodology for vehicular flocking in lane-free traffic. (Color online only.)

$$x_i(k+1) = x_i(k) + Tv_{i,x}(k) + \frac{1}{2}T^2u_{i,x}(k) \quad (1a)$$

$$v_{i,x}(k+1) = v_{i,x}(k) + Tu_{i,x}(k) \quad (1b)$$

$$y_i(k+1) = y_i(k) + Tv_{i,y}(k) + \frac{1}{2}T^2u_{i,y}(k) \quad (1c)$$

$$v_{i,y}(k+1) = v_{i,y}(k) + Tu_{i,y}(k) \quad (1d)$$

where  $x_i$  and  $v_{i,x}$  are the longitudinal position and speed of the vehicle, whereas  $y_i$  and  $v_{i,y}$  represent the lateral position and speed, and  $u_{i,x}$  and  $u_{i,y}$  are the longitudinal and lateral accelerations, respectively. In Equation 1,  $T$  is the sampling period and  $k = 0, 1, \dots$  is the discrete-time index where  $t = k \cdot T$ . Note that the vehicle states are measured with respect to the vehicle's center. The motion dynamics (Equation 1) are subject to the following bound constraints:

$$-u_{x, \min} < u_{i,x}(k) < u_{x, \max} \quad (2a)$$

$$-u_{y, \min} < u_{i,y}(k) < u_{y, \max} \quad (2b)$$

$$v_{i,y}(k) < \alpha_l \cdot v_{i,x}(k) \quad (2c)$$

The longitudinal and lateral acceleration of vehicles are limited because of the physical capability of the vehicles for accelerating and braking and, of course, because of the comfort issues of the passengers. In addition, since the movement of vehicles, specifically in highways, is essentially longitudinal, the decoupled Equation 1 is justified (28). However, to prevent inappropriate lateral maneuvers, the lateral speed is assumed to be bounded by the longitudinal speed as in Equation 2c, where  $\alpha_l$  is a tuning parameter.

**Flock Topology.** The vehicle flock topology is modeled as a spatial graph. A graph  $G = (V, E)$  consists of a set of vertices (or nodes)  $V = \{1, 2, \dots, n\}$  and edges (or links)  $E \subseteq \{(i, j) | i, j \in V, j \neq i\}$ . A graph is undirected if  $(i, j) \in E \Leftrightarrow (j, i) \in E$  (44). The adjacency matrix  $A = [a_{ij}]$  of a graph is a matrix with 0-1 elements satisfying the property  $a_{ij} \neq 0 \Leftrightarrow (i, j) \in E$ . In this work, we assume a

weighted adjacency matrix for the vehicle flock whose non-zero elements are position-dependent. Therefore, the induced graph is dynamic or is called a spatial graph. More specifically, each vehicle is one vertex of the graph and  $a_{ij}$  is defined as the elliptic distance between the two vehicles  $i$  and  $j$  using the following equations:

$$a_{ij} = \sqrt{\left(\frac{dx_{ij}}{e_a}\right)^2 + \left(\frac{dy_{ij}}{e_b}\right)^2} \quad (3)$$

where  $e_a$  and  $e_b$  are the elliptic distance parameters and  $dx_{ij} = x_i - x_j$  and  $dy_{ij} = y_i - y_j$  are the longitudinal and lateral space gaps between the two vehicles, respectively. With this definition, the adjacency matrix will be symmetric ( $A^T = A$ ). The adjacency matrix is used later in Equation 9 in the consensus algorithm, a component of the flocking algorithm, where each vehicle  $j$  contributes to the change in the speed of vehicle  $i$  with the factor of  $a_{ij}$ .

### Flocking Algorithm

The flocking algorithm consists of three terms and is inspired by the work of Olfati-Saber (41). In his flocking theory, three types of agents are considered:  $\alpha$ -agents,  $\beta$ -agents, and  $\gamma$ -agents, which represent agents performing flocking, obstacles, and (virtual) collective objectives or leaders, respectively. In this present work, we only consider the  $\alpha$ - and  $\gamma$ -agents. Since the focus of this paper is on the vehicular flock formation and analysis of its behavior, no obstacle is considered. Note that the collision avoidance between the flock members is addressed by means of the defined energy function and the corresponding gradient-based term. In addition, for controlling the flock within the boundary, a boundary control approach that limits the lateral acceleration of the vehicles is proposed. The flocking behavior of the  $\alpha$ -agents is controlled using the gradient of the proposed energy function and a consensus algorithm. The consideration of a virtual leader, the  $\gamma$ -agent, controls the collective behavior of the flock. Thus, the control input of vehicle  $i$  in each direction has three terms:

$$u_{i,x} = c_g \cdot f_{i,x}^g + c_c \cdot f_{i,x}^c + c_\gamma \cdot f_{i,x}^\gamma, \quad (4a)$$

$$u_{i,y} = c_g \cdot f_{i,y}^g + c_c \cdot f_{i,y}^c + c_\gamma \cdot f_{i,y}^\gamma, \quad (4b)$$

where  $f^g$  is the gradient-based term,  $f^c$  is the consensus term, and  $f^\gamma$  is the navigational feedback imposed by the virtual leader or  $\gamma$ -agent. The contribution of each term in the final applied acceleration is defined based on the weighting factors  $c_g$ ,  $c_c$ , and  $c_\gamma$ . The different terms are visualized in the bottom part of Figure 2. The flowchart uses the same colors as the schematic representation in the top part with the red vehicle depicting the currently

considered ego vehicle  $i$ . As described above, the current longitudinal and lateral positions and speeds of all vehicles are known. Now, the relative positions to other  $\alpha$ -agents are used in the flock centering term (green box) to derive  $f_i^g$ . The consensus term (purple box) uses the speed differences between vehicles in the neighborhood defined by the adjacency matrix to derive  $f_i^c$ . The trajectory of the  $\gamma$ -agent and the attempt of the flock to follow this virtual leader provides  $f_i^\gamma$ . Before the acceleration  $u_i$  obtained from Equation 4 is applied in the next time step, it is limited by the boundary control (yellow box) and kinematic limitations. In the following sections, each part is elaborated in detail.

**Definition of the Energy Function and Its Gradient.** As mentioned in the background section, three simple rules define the collective behavior of a flock (32). In this paper, by defining a proper energy function, the first two Reynolds rules, that is, flock centering and collision avoidance with flock members, are realized. To this end, the two-dimensional Mexican hat function, originally proposed by Ricker (45) to describe the propagation of seismic waves, is used to model the energy function:

$$\varphi(x, y) = M \cdot \left( 1 - k_1 \cdot \left( \left( \frac{x}{f_a} \right)^2 + \left( \frac{y}{f_b} \right)^2 \right) \right) \cdot \exp\left( -k_2 \cdot \left( \left( \frac{x}{f_a} \right)^2 + \left( \frac{y}{f_b} \right)^2 \right) \right) \quad (5)$$

where  $f_a$  and  $f_b$  define the shape and location of the minimum area of the function in the longitudinal and lateral directions, respectively, and  $M$ ,  $k_1$ , and  $k_2$  are tuning parameters to scale the function. The function with two sets of parameter values is shown in Figure 3a. The proposed energy function has a clear ellipsoid area with minimum energy shown in a bluish color. In addition, it is shown how the size and shape of the minimum area are affected by the change of the function variables. Note that the shape of the energy function defines the location of the vehicles in the flock, since the vehicles move toward the locations with the minimum energy. The area outside this ellipse implies the attraction force and the area inside repels the other flock members. For a better understanding of the shape of the energy function, a three-dimensional view of it is illustrated in Figure 3b.

The values of  $f_a$  and  $f_b$  are a function of the vehicles' size, the flock speed, and the initial distribution of the vehicles. In the case in which the vehicles are initially far from each other, a larger attraction region is required and, as long as the vehicles approach each other,  $f_a$  and  $f_b$  take smaller values allowing closer space gaps between the flock members. In addition, as the flock speed increases, the repulsion area should expand for safety reasons.

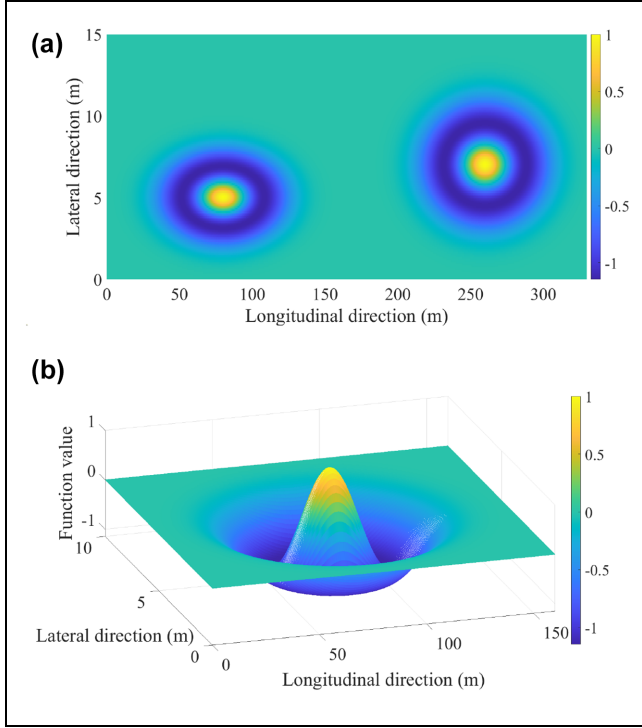


**Figure 3.** The Mexican hat function is used as the energy function for flock formation: (a) top view of two Mexican hat functions and (b) three-dimensional view of a Mexican hat function. (Color online only.)

Each vehicle  $i$  has its own energy function and applies a flocking force in the negative direction of its energy function gradient  $f_i^g = -\nabla\varphi(x, y)$  to other flock members. The gradient of the Mexican hat function is  $\nabla\varphi(x, y) = \frac{\partial\varphi}{\partial x}(x, y)\vec{x} + \frac{\partial\varphi}{\partial y}(x, y)\vec{y}$ . Here,  $\vec{x}$  indicates the longitudinal direction and  $\vec{y}$  refers to the lateral one. The partial derivatives are calculated as follows:

$$\frac{\partial\varphi}{\partial x}(x, y) = \frac{x}{f_a^2} \cdot CT \quad (6a)$$

$$\frac{\partial\varphi}{\partial y}(x, y) = \frac{y}{f_b^2} \cdot CT \quad (6b)$$

where  $CT$  is the common term used in both partial derivatives and is calculated as follows:

$$CT = -2Mk_1 \exp\left(-k_2 \left(\left(\frac{x}{f_a}\right)^2 + \left(\frac{y}{f_b}\right)^2\right)\right) \cdot \left(1 + \frac{k_2}{k_1} \left(1 - k_1 \left(\left(\frac{x}{f_a}\right)^2 + \left(\frac{y}{f_b}\right)^2\right)\right)\right) \quad (7)$$

For any vehicle  $i$  at time  $k$ , the gradient-based force is calculated as shown in Equation 8 for the longitudinal and lateral directions:

$$f_{i,x}^g = -\sum_{j=1}^n \frac{\partial\varphi}{\partial x}(dx_{ij}, dy_{ij}), j \neq i \quad (8a)$$

$$f_{i,y}^g = -\sum_{j=1}^n \frac{\partial\varphi}{\partial y}(dx_{ij}, dy_{ij}), j \neq i \quad (8b)$$

where  $n$  is the number of flock members. Obviously, the closer neighboring vehicles have a higher effect on the vehicle. This is completely in line with the flock centering rule of Reynolds. The rule states that each individual attempts to stay close to nearby flockmates, which therefore have a large influence, while the actual center of the entire flock is unknown to the individual (32).

**Consensus Algorithm.** In this work, the third Reynolds rule (32), that is, the velocity matching of the flock members, is carried out using the consensus algorithm in both longitudinal and lateral directions. In networks of agents (or dynamic systems), “consensus” means to achieve an agreement on a single target value with respect to a certain quantity of interest that depends on the state of all agents (40). In the following consensus algorithm, the speed of the vehicle is affected by the speed of other vehicles with the factor of their corresponding adjacency element. In Equation 9, we additionally normalize the consensus term to keep its value consistent with the other flocking terms in Equation 4. This approach leads to minimum variation in vehicle speeds within the flock. This implementation does not only harmonize the flock speed, but also dampens the speed perturbation of the flock members:

$$f_{i,x}^c = \frac{\sum_{j=1}^n a_{ij}(v_{j,x} - v_{i,x})}{\sum_{j=1}^n a_{ij}} \quad (9a)$$

$$f_{i,y}^c = \frac{\sum_{j=1}^n a_{ij}(v_{j,y} - v_{i,y})}{\sum_{j=1}^n a_{ij}} \quad (9b)$$

where  $a_{ij}$  is the corresponding elliptic distance defined in Equation 3.

**Navigational Feedback via a Virtual Leader.** In addition to the location of vehicles in the flock and their relative speed, the overall path and movement of a vehicular flock should be controlled for several reasons, such as traffic efficiency and traffic measure purposes. To this end, a “virtual” leader as the  $\gamma$ -agent is defined whose longitudinal speed and lateral movement (defined by the lateral speed) are defined in an upper-level controller. The longitudinal and lateral speed of this leader are used in the flocking control algorithm to shape the collective goal of the flock. Note that the lateral location of the vehicles should not be similar to the lateral location of the  $\gamma$ -agent so as to prevent platoon behavior. The derived

desired trajectory plays the role of navigational feedback and helps the flock navigate through curves and so forth, or dampen traffic shockwaves by longitudinal acceleration or deceleration.

We assume that the dynamics of the virtual leader also follow the double integrator model given in Equation 1. Thus, the  $\gamma$ -agent force in Equation 4 is calculated as follows:

$$f_{i,x}^{\gamma} = c_1(v_{\gamma,x} - v_{i,x}) \quad (10)$$

$$f_{i,y}^{\gamma} = c_2(v_{\gamma,y} - v_{i,y}) \quad (11)$$

where  $c_1$  and  $c_2$  are control gains.

### Dynamic Boundary Control

It is crucial to bound the movement of all vehicles within the road boundary. In addition, a flock should not occupy the full lateral occupancy of the road. The boundary of the flock should be controlled, specifically when the flock should follow a pre-defined path to perform an overtaking maneuver or allow an emergency vehicle preemption, as indicated in Figure 1. Therefore, the need for efficient boundary control for the flock is essential. To this end, additional lateral acceleration constraints are required. This task may be addressed as a feedback control problem, whereby the left (right) road boundary is considered a reference value for all vehicles' lateral movement (46). This control command specifies how much lateral acceleration is needed to lead the vehicle toward the boundary. This value is then assumed as the maximum acceleration and ensures that the vehicles never cross the boundary.

Assuming that  $w$  is the vehicle width and  $y_l(k)$  and  $y_r(k)$ , where  $y_l(k) > y_r(k)$ , are the left and right road boundary, respectively, the left (right) desired reference location for the boundary control is  $y_{b,l}(k) = y_l(k) - w/2$  ( $y_{b,r}(k) = y_r(k) + w/2$ ). Given that the road geometry information is known, we consider that the lateral speed  $v_{b,l}(k)$  ( $v_{b,r}(k)$ ) at which the location of the left (right) road boundary changes at time  $k$  is also known. We now consider the following set of state-feedback (left and right) boundary controllers for the lateral acceleration of the vehicle  $i$  developed by Malekzadeh et al. (46) with the extension that, in our case, the boundary changes dynamically and thus  $v_{b,l}$  ( $v_{b,r}$ ) is non-zero:

$$b_{i,l}^{acc} = b_1(y_{b,l} - y_{i,y}) + b_2(v_{b,l} - v_{i,y}) \quad (12)$$

$$b_{i,r}^{acc} = b_1(y_{b,r} - y_{i,y}) + b_2(v_{b,r} - v_{i,y}) \quad (13)$$

where  $b_1$  and  $b_2$  are feedback gains. As mentioned earlier, these lateral accelerations bound the vehicles' acceleration. Therefore, the bound constraint (Equation 2b) is updated as follows:

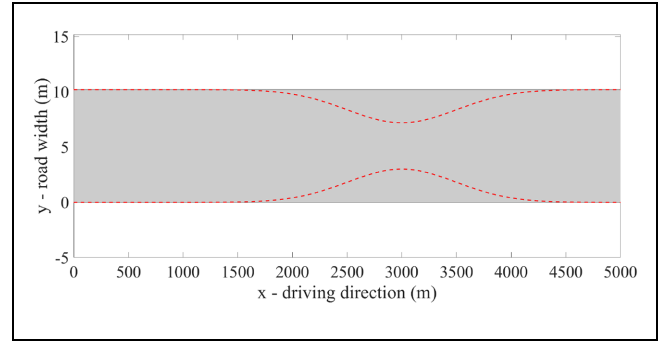


Figure 4. An overview of the considered traffic network. (Color online only.)

$$\max(b_{i,r}^{acc}, -u_{y, \min}) < u_{i,y}(k) < \min(b_{i,l}^{acc}, u_{y, \max}) \quad (14)$$

Note that the input arguments in the *minimum* function in Equation 14 have positive values, whereas the *maximum* function applies on the negative arguments.

### Simulation Setup

To evaluate the proposed approach, a stretch of a ring road with 5 km length and 10.2 m width is developed in the software MATLAB as the traffic network. This network is illustrated in Figure 4. In addition to the permanent road boundary, a new dynamic flock boundary is defined that restricts the lateral movement of the flock. This boundary could be the result of a bottleneck, construction site, emergency vehicle preemption, or any other obstacle. The flock boundary is shown with a dashed red line in Figure 4. At the beginning of the simulation, vehicles are positioned randomly at the first section of the road with different initial speeds. For the  $\gamma$ -agent, we assume a pre-defined and known trajectory.

Without loss of generality and for the simplicity of evaluating the results, we assume five vehicles with random initial locations and random initial longitudinal speeds in the range of 15–35 m/s. The simulation duration is 5 min. The simulation results are shown and evaluated in the next section.

### Results and Discussion

The simulation results are presented in the following with each section focusing on a different aspect. Firstly, it is shown how different input values and road boundaries lead to different flock formations. Secondly, the effect of the consensus algorithm is demonstrated. Afterwards, the impacts of the  $\gamma$ -agent are described before the stability of the flock against perturbations is demonstrated.



### Flock Formation

Firstly, the results of the flock formation are shown in this section for three different scenarios. Within the first scenario, an energy function with a larger ellipsoid area is chosen. The second scenario uses the same energy function, but exhibits a squeezed road boundary because of the possible use cases mentioned above (e.g., bottleneck). The third scenario uses an energy function with a smaller ellipsoid area under normal road boundaries. Figure 5 shows for all of the three mentioned scenarios that the implemented flocking algorithm successfully leads to the formation of vehicular flocks in lane-free traffic. In the figures, a flock of five vehicles is shown for each scenario. The size of the flock is also depicted. Note that, for consistency in the rest of this section, the vehicle numbering and coloring remain the same, as shown in Figure 5a. The figures clearly depict that, as intended, the vehicle arrangement within the flock formation remains the same in all scenarios, and only the longitudinal and lateral space gaps between vehicles, or consequently the flock size, change with changing boundaries or different sizes of the energy function. The values of  $f_a$  and  $f_b$  of the Mexican hat function in Figure 5c are smaller compared to the ones in Figure 5a. Consequently, scenario 3 exhibits a smaller ellipsoid area compared to scenario 1. Therefore, the size of the flock and the longitudinal and lateral space gaps between vehicles are also smaller. This demonstrates that the energy functions defined in Equation 5 fulfill the flock centering requirements. In scenario 2, the boundary of the ring road was squeezed by 3 m at both sides, for example, because of a bottleneck. Figure 5b reveals the effect of the squeezed boundary on the lateral size of the flock. Also here, the vehicle arrangement is stable but longitudinal and lateral space gaps are adjusted.

### Velocity Matching

As mentioned in the methodology section, the consensus algorithm is used to perform the velocity matching of the flock. The longitudinal speeds of the vehicles at the very beginning of the simulation time are shown in Figure 6a. Initially, vehicles take different random speeds between 15 and 35 m/s, and just after a few seconds, they approach the agreed speed, which is, in this case, the speed of the  $\gamma$ -agent. The lateral speed of the vehicles at the similar simulation time is shown in Figure 6b. This clearly demonstrates that the implemented consensus algorithm successfully aligns longitudinal speeds between vehicles.

The vehicles' initial lateral speed is zero and changes at the very first seconds because of the flock formation induced by the gradient-based term (see Equation 8).

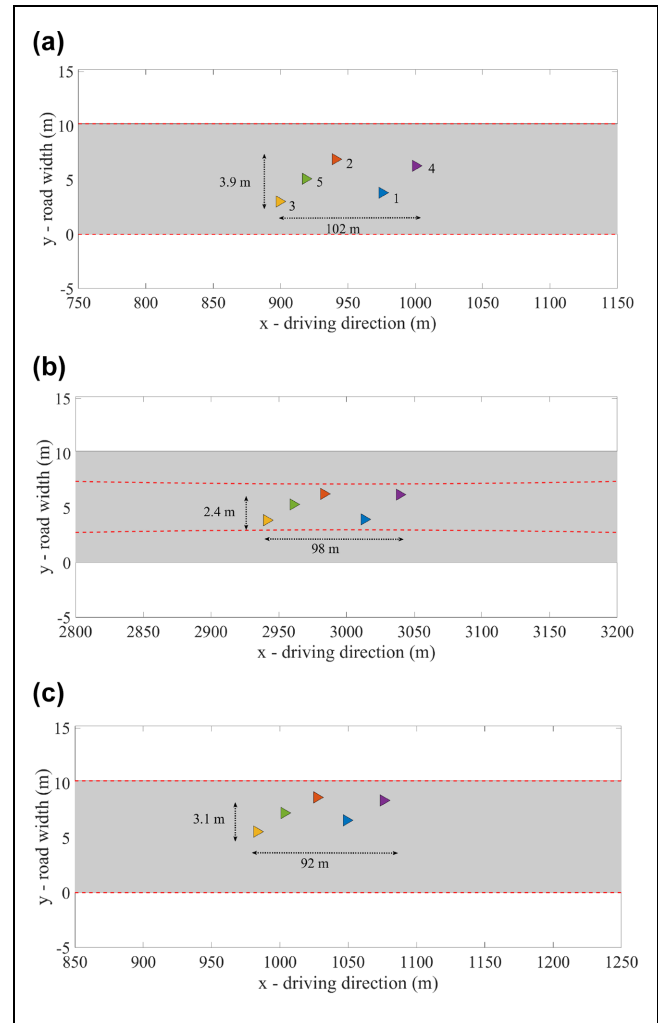


**Figure 5.** The location of vehicles within the flock depends on the size of the Mexican hat function and the road boundary: (a) location of vehicles with larger energy function (scenario 1), (b) location of vehicles at the squeezed boundary (scenario 2), and (c) location of vehicles with a smaller energy function (scenario 3). (Color online only.)

This fast convergence of the lateral speed also demonstrates the effectiveness of the used energy function.

### Navigational Feedback

The third term in the flocking algorithm is based on the virtual leader, the  $\gamma$ -agent, and its trajectory. The effect of the  $\gamma$ -agent's speed is partially illustrated in Figure 6, where the flock vehicles agree and converge to its speed. However, and for better evaluation of the navigational feedback, we assumed a pre-defined trajectory for the  $\gamma$ -agent that should be followed by the flock. Figure 7 shows how the vehicles' longitudinal and lateral speeds follow the speed of the virtual leader. The speed of the

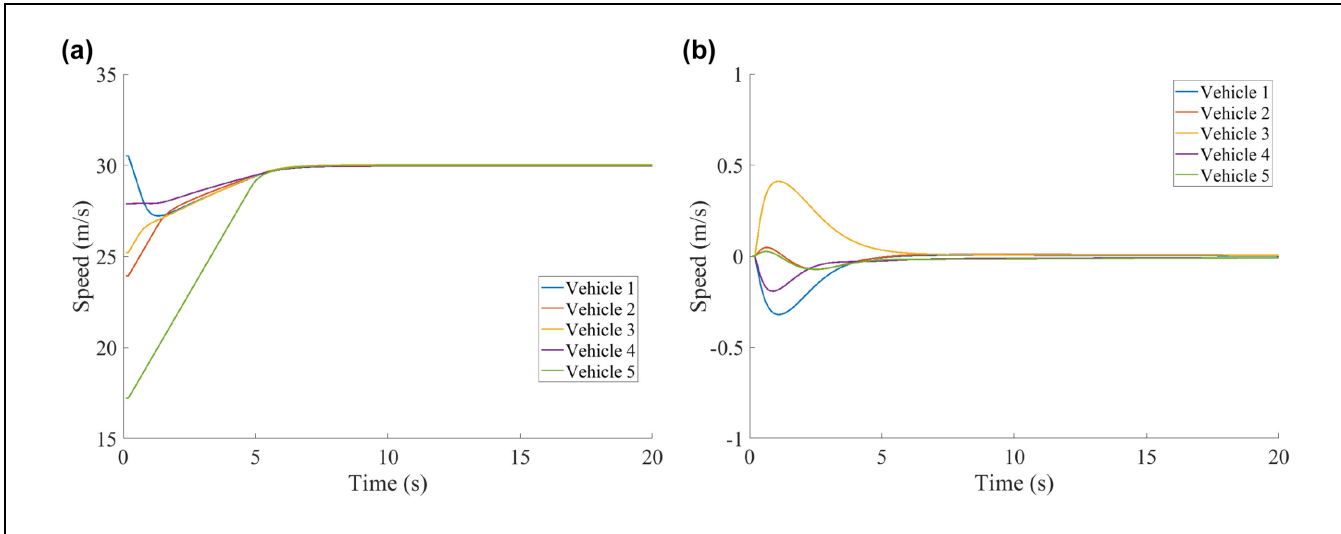


**Figure 6.** All the vehicles agree on a similar speed as the result of the flocking algorithm: (a) longitudinal speed of the vehicles and (b) lateral speed of the vehicles.

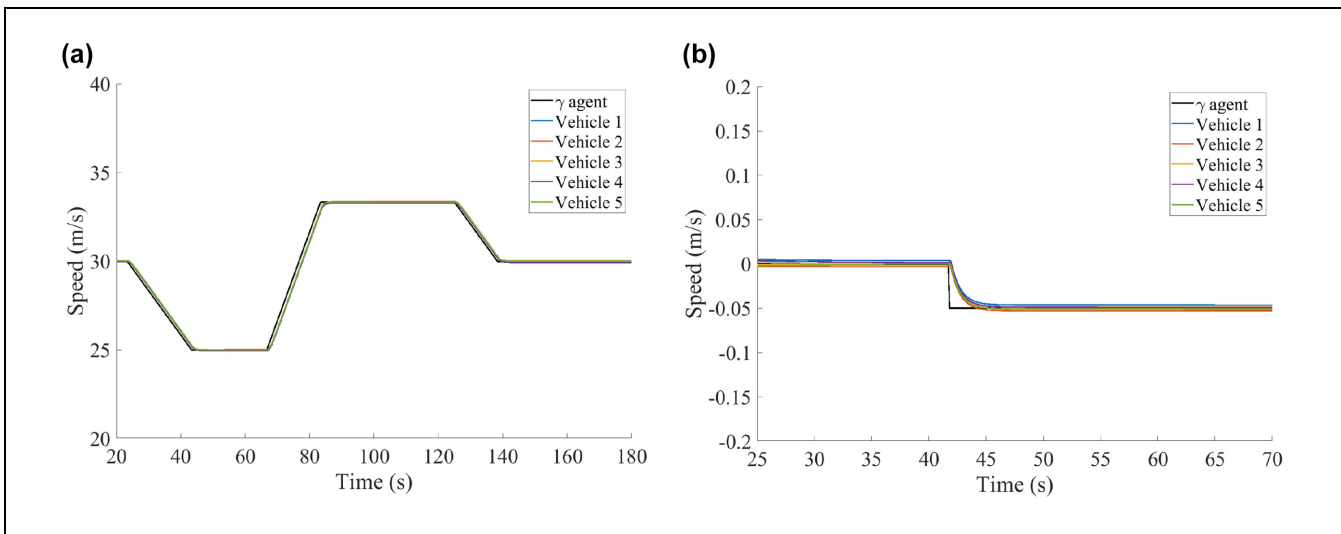


**Figure 7.** The speed of the vehicles follows the dynamics of the  $\gamma$ -agent: (a) longitudinal speed of the vehicles and (b) lateral speed of the vehicles.

virtual leader is defined in an upper-level controller, for example based on the downstream traffic conditions. This feature allows the implementation of a speed limit for the flock or shockwave dampening strategies via vehicular flocking.

In addition to that, in Figure 8, the lateral movement of all vehicles, as well as of the  $\gamma$ -agent, are shown and compared over time. Initially, the lateral position of the  $\gamma$ -agent does not change. After a few seconds of the flock formation phase, vehicles maintain their lateral location and then follow the path defined by the movement of the  $\gamma$ -agent. This trajectory following is a desired behavior of the flock with many use cases. For

instance, the virtual leader could navigate vehicles through curves or construction zones, make the flock move to the side to let an emergency vehicle pass, lead the flock on energy-efficient trajectories, or even coordinate overtaking maneuvers. Note that the vehicles roughly pass the bottleneck between seconds 75 and 105 of the simulation. Although vehicles have different longitudinal positions and arrive at the bottleneck with some short delays, in Figure 8 we show how the bottleneck affects the lateral locations of vehicles. During this time, the lateral locations of the vehicles, as already discussed, are imposed by the dynamic boundary constraints. Following the bottleneck, the vehicles follow the  $\gamma$ -agent

trajectory, again demonstrating the stability of the implementation under different scenarios.

**Flock Stability**

Finally, we demonstrate the stability of the flock in the case of perturbation. At the time of 200 s, manual

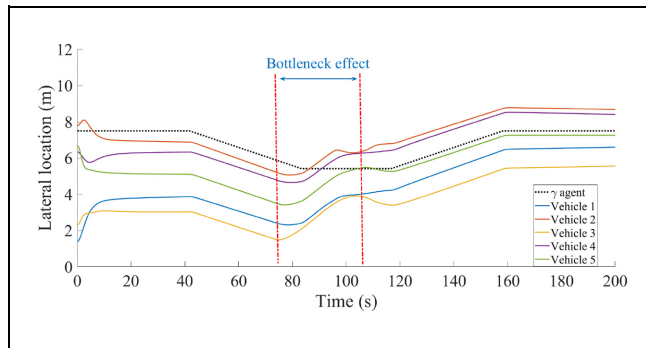


**Figure 8.** The lateral location of the vehicles follows the lateral movement of the  $\gamma$ -agent.

braking is applied to the front vehicle, that is, vehicle number 4. This braking is implemented by exerting a longitudinal deceleration of  $-2\text{ m/s}^2$  for a duration of 1 s. In Figure 9, the consequences of this perturbation on the other vehicles' longitudinal and lateral accelerations and speeds are depicted. The results in Figure 9, *a* and *b*, shows that once the perturbation signal is released to vehicle 4, it takes the maximum possible longitudinal acceleration to recover its previous speed. More interestingly, it is noticeably visible that the other vehicles encounter tiny longitudinal acceleration and speed changes, demonstrating that the induced shock is dampened very efficiently. The dampening behavior is also illustrated in Figure 9, *c* and *d*, where the lateral acceleration and speed of the vehicles are shown. The flexibility of the vehicles within lane-free traffic to slightly change their lateral location compared to lane-based traffic reduces the negative and large longitudinal effect of the perturbation on the rear vehicles. In particular, the front vehicle, vehicle 4, and its predecessor, vehicle 1, drive in the opposite directions, alleviating the longitudinal perturbation consequences.

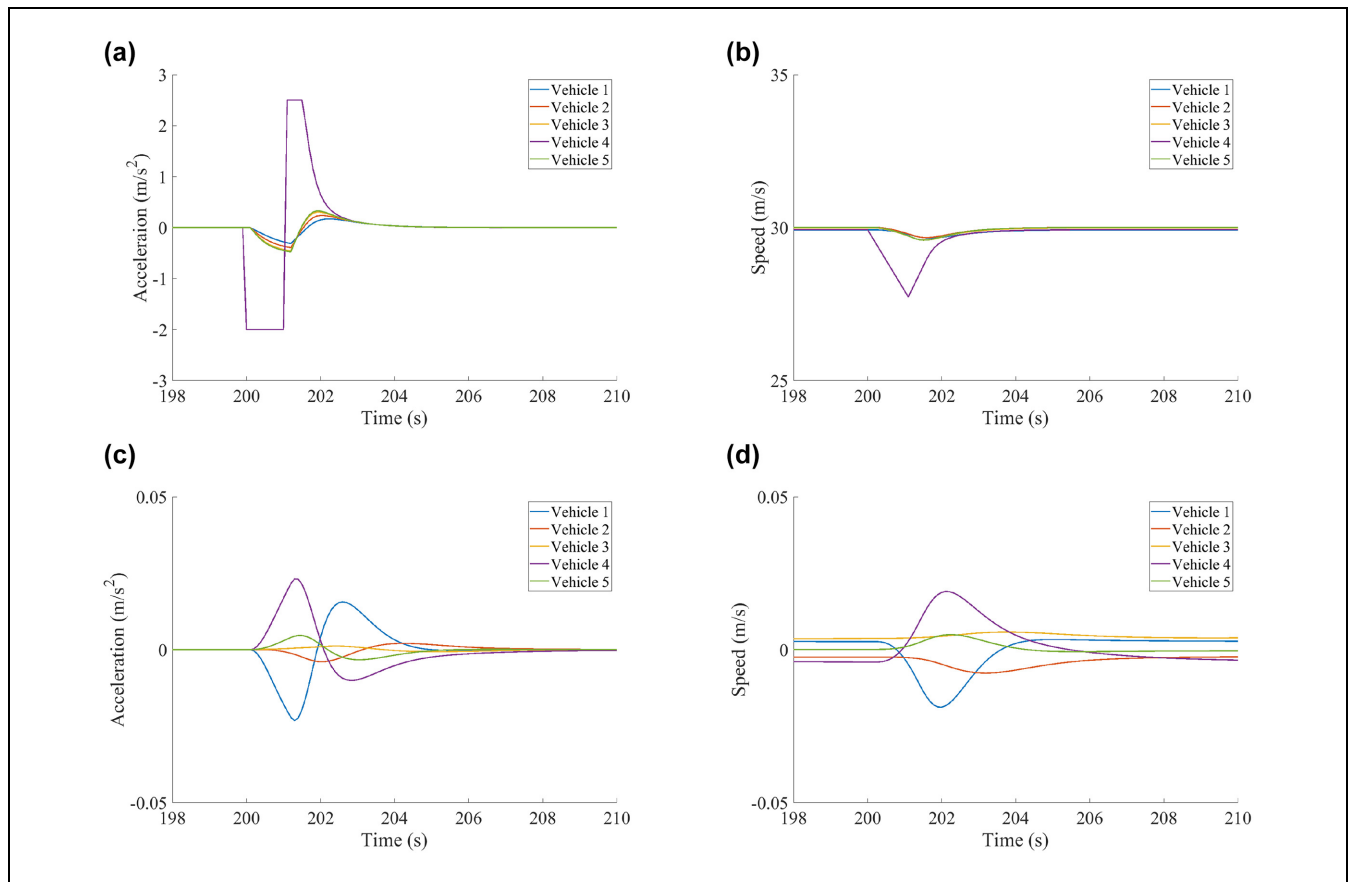


**Figure 9.** The vehicles go back to their equilibrium condition after the perturbation: (a) longitudinal acceleration of the vehicles, (b) longitudinal speed of the vehicles, (c) lateral acceleration of the vehicles, and (d) lateral speed of the vehicles.

## Conclusion

Within this paper, we developed a new control algorithm for the flocking of automated vehicles in lane-free traffic that allows for achieving certain speeds, vehicle headways, and lateral distributions of vehicles on the road. The flocking algorithm is inspired by the work of Olfati-Saber et al. (40) and considers two types of agents:  $\alpha$ -agents that represent vehicles performing flocking and  $\gamma$ -agents that represent virtual leaders with collective objectives (e.g., slowing down in the case of traffic congestion ahead or following specific energy-efficient trajectories). Since the focus of this paper was on the implementation and analysis of flock formations, no obstacles ( $\beta$ -agents) were considered yet. For the  $\alpha$ -agents, we defined a specific type of energy function that resulted in attraction and repulsion forces outside and inside of an ellipsoid area around the vehicle, respectively. Thereby, we successfully implemented the flock centering and collision avoidance rules. The velocity matching was realized by applying a normalized consensus algorithm, which not only harmonizes the flock speed, but also dampens the speed perturbation of the flock members. The following of the virtual leader's trajectory, defined in an upper-level controller, was realized via the  $\gamma$ -agent concept and the implemented navigational feedback. Finally, a feedback control algorithm was implemented for the dynamic boundary control.

The proposed approach was simulated for different scenarios within the software MATLAB with very promising results. Vehicular flocks were successfully and efficiently formed via energy functions within a few seconds and speeds aligned by the consensus algorithm. The flocks showed stable vehicle arrangements but changing sizes depending on the chosen energy functions and road boundaries. It was also demonstrated that the vehicles follow the trajectory of the virtual leader. Most importantly, we demonstrated the stability of the flock in the case of perturbation caused by a braking vehicle. The induced shock is dampened very efficiently as the vehicles are more flexible to slightly change their lateral location, which reduces the required longitudinal acceleration and speed changes.

Within future research, we would like to integrate an obstacle avoidance mechanism into our control algorithm. This allows us to implement the flock formation and movement in real traffic conditions with other non-flock vehicles. Until now, we did not control for specific vehicle arrangements within the flock, for example, to further minimize the aerodynamic drag in the case of side winds. This could be done by varying the orientations of the energy functions or by applying additional forces pushing the flock members to fixed positions inside the group. We also plan to implement the proposed flocking method within the traffic simulator SUMO. The implementation of flocks in a realistic traffic simulator paves

the way for the evaluation of the impact of the flock formation on the road capacity and, additionally, exploitation of the flock as the traffic control measure.

## Author Contributions

The authors confirm contribution to the paper as follows: study conception and design: M. Rostami-Shahrbabaki, S. Weikl, T. Niels, K. Bogenberger; data collection: M. Rostami-Shahrbabaki; analysis and interpretation of results: M. Rostami-Shahrbabaki, S. Weikl, T. Niels; draft manuscript preparation: M. Rostami-Shahrbabaki, S. Weikl, T. Niels, K. Bogenberger. All authors reviewed the results and approved the final version of the manuscript.

## Declaration of Conflicting Interests


The author(s) declared no potential conflicts of interest with respect to the research, authorship, and/or publication of this article.


## Funding


The author(s) disclosed receipt of the following financial support for the research, authorship, and/or publication of this article: This work is based on the project "Simulation and organization of future lane-free traffic" funded by the German research foundation (DFG), under the project number BO 5959/1-1.

## ORCID iDs

Majid Rostami-Shahrbabaki  <https://orcid.org/0000-0002-8129-4519>

Simone Weikl  <https://orcid.org/0000-0003-2724-8578>

Tanja Niels  <https://orcid.org/0000-0002-8530-0285>

Klaus Bogenberger  <https://orcid.org/0000-0003-3868-9571>

## References

1. Kavathekar, P., and Y. Chen. Vehicle Platooning: A Brief Survey and Categorization. *Proc., International Design Engineering Technical Conferences and Computers and Information in Engineering Conference*, Vol. 54808, Washington, D.C., ASME, 2011, pp. 829–845.
2. Németh, B., and P. Gáspár. Optimised Speed Profile Design of a Vehicle Platoon Considering Road Inclinations. *IET Intelligent Transport Systems*, Vol. 8, No. 3, 2014, pp. 200–208.
3. Johansson, I., J. Jin, X. Ma, and H. Pettersson. Look-Ahead Speed Planning for Heavy-Duty Vehicle Platoons Using Traffic Information. *Transportation Research Proceedings*, Vol. 22, 2017, pp. 561–569.
4. Wang, M., S. Maarseveen, R. Happee, O. Tool, and B. Arem. Benefits and Risks of Truck Platooning on Freeway Operations Near Entrance Ramp. *Transportation Research Record: Journal of the Transportation Research Board*, 2019. 2673: 588–602.
5. Papageorgiou, M., K. Mountakis, I. Karafyllis, I. Papamichail, and Y. Wang. Lane-Free Artificial-Fluid Concept

- for Vehicular Traffic. *Proceedings of the IEEE*, Vol. 109, 2021, pp. 114–121.
6. Berahman, M., M. Rostami-Shahrbabaki, and K. Bogenberger. Driving Strategy for Vehicles in Lane-Free Traffic Environment Based on Deep Deterministic Policy Gradient and Artificial Forces. *IFAC-PapersOnLine*, Vol. 55, No. 14, 2022, pp. 14–21.
  7. Rostami-Shahrbabaki, M., S. Weikl, M. Akbarzadeh, and K. Bogenberger. A Two-Layer Approach for Vehicular Flocking in Lane-Free Environment. *Proc., 11th Triennial Symposium on Transportation Analysis (TRISTAN)*, Mauritius, Island, 2022.
  8. Ngoduy, D. Platoon-Based Macroscopic Model for Intelligent Traffic Flow. *Transportmetrica B: Transport Dynamics*, Vol. 1, 2013, pp. 153–169.
  9. Kaluva, S., A. Pathak, and A. Ongel. Aerodynamic Drag Analysis of Autonomous Electric Vehicle Platoons. *Energies*, Vol. 13, 2020, p. 4028.
  10. Tsugawa, S., S. Jeschke, and S. Shladover. A Review of Truck Platooning Projects for Energy Savings. *IEEE Transactions on Intelligent Vehicles*, Vol. 1, 2016, pp. 68–77.
  11. Bhoopalam, A., N. Agatz, and R. Zuidwijk. Planning of Truck Platoons: A Literature Review and Directions for Future Research. *Transportation Research Part B: Methodological*, Vol. 107, 2018, pp. 212–228.
  12. Xiao, L., and F. Gao. Practical String Stability of Platoon of Adaptive Cruise Control Vehicles. *IEEE Transactions on Intelligent Transportation Systems*, Vol. 12, 2011, pp. 1184–1194.
  13. Feng, S., Y. Zhang, S. Li, Z. Cao, H. Liu, and L. Li. String Stability for Vehicular Platoon Control: Definitions and Analysis Methods. *Annual Reviews in Control*, Vol. 47, 2019, pp. 81–97.
  14. Shladover, S., C. Nowakowski, X. Lu, and R. Ferlis. Cooperative Adaptive Cruise Control: Definitions and Operating Concepts. *Transportation Research Record: Journal of the Transportation Research Board*, 2015. 2489: 145–152.
  15. Kato, S., S. Tsugawa, K. Tokuda, T. Matsui, and H. Fujii. Vehicle Control Algorithms for Cooperative Driving with Automated Vehicles and Intervehicle Communications. *IEEE Transactions on Intelligent Transportation Systems*, Vol. 3, 2002, pp. 155–161.
  16. Gao, L., D. Chu, Y. Cao, L. Lu, and C. Wu. Multi-Lane Convoy Control for Autonomous Vehicles Based on Distributed Graph and Potential Field. *Proc., IEEE Intelligent Transportation Systems Conference (ITSC)*, IEEE, New York, 2019, pp. 2463–2469.
  17. Caruntu, C., L. Ferariu, C. Pascal, N. Cleju, and C. Comsa. Connected Cooperative Control for Multiple-Lane Automated Vehicle Flocking on Highway Scenarios. *Proc., 23rd International Conference on System Theory, Control and Computing (ICSTCC)*, IEEE, New York, 2019, pp. 791–796.
  18. Caruntu, C., A. Maxim, and R. Rafaila. Multiple-Lane Vehicle Platooning Based on a Multi-Agent Distributed Model Predictive Control Strategy. *Proc., 22nd International Conference on System Theory, Control and Computing (ICSTCC)*, IEEE, New York, 2018, pp. 759–764.
  19. Caruntu, C., L. Ferariu, C. Pascal, N. Cleju, and C. Comsa. A Concept of Multiple-Lane Vehicle Grouping by Swarm Intelligence. *Proc., 24th IEEE International Conference on Emerging Technologies and Factory Automation (ETFA)*, IEEE, New York, 2019, pp. 1183–1188.
  20. Wang, F., and Y. Chen. A Novel Hierarchical Flocking Control Framework for Connected and Automated Vehicles. *IEEE Transactions on Intelligent Transportation Systems*, Vol. 22, 2020, pp. 4801–4812.
  21. Hao, R., M. Liu, W. Ma, B. Van Arem, and M. Wang. A Flock-Like Two-Dimensional Cooperative Vehicle Formation Model Based on Potential Functions. *Transportmetrica B: Transport Dynamics*, Vol. 11, 2023, pp. 174–195.
  22. Xu, Q., M. Cai, K. Li, B. Xu, J. Wang, and X. Wu. Coordinated Formation Control for Intelligent and Connected Vehicles in Multiple Traffic Scenarios. *IET Intelligent Transport Systems*, Vol. 15, 2021, pp. 159–173.
  23. Sekeran, M., M. Rostami-Shahrbabaki, A. Syed, M. Margreiter, and K. Bogenberger. Lane-Free Traffic: History and State of the Art. *Proc., IEEE 25th International Conference on Intelligent Transportation Systems (ITSC)*, IEEE, New York, 2022, pp. 1037–1042.
  24. Malekzadeh, M., I. Papamichail, and M. Papageorgiou. Linear–Quadratic Regulators for Internal Boundary Control of Lane-Free Automated Vehicle Traffic. *Control Engineering Practice*, Vol. 115, 2021, p. 104912.
  25. Malekzadeh, M., I. Papamichail, M. Papageorgiou, and K. Bogenberger. Optimal Internal Boundary Control of Lane-Free Automated Vehicle Traffic. *Transportation Research Part C: Emerging Technologies*, Vol. 126, 2021, p. 103060.
  26. Levy, R., and J. Haddad. Path and Trajectory Planning for Autonomous Vehicles on Roads Without Lanes. *Proc., IEEE International Intelligent Transportation Systems Conference (ITSC)*, IEEE, New York, 2021, pp. 3871–3876.
  27. Karafyllis, I., D. Theodosis, and M. Papageorgiou. Lyapunov-Based Two-Dimensional Cruise Control of Autonomous Vehicles on Lane-Free Roads. *Proc., 60th IEEE Conference on Decision and Control (CDC)*, IEEE, Austin, TX, 2021, pp. 2683–2689.
  28. Yanumula, V., P. Typaldos, D. Troullinos, M. Malekzadeh, I. Papamichail, and M. Papageorgiou. Optimal Path Planning for Connected and Automated Vehicles in Lane-Free Traffic. *Proc., IEEE International Intelligent Transportation Systems Conference (ITSC)*, Indianapolis, IN, 2021, pp. 3545–3552.
  29. Troullinos, D., G. Chalkiadakis, I. Papamichail, and M. Papageorgiou. Collaborative Multiagent Decision Making for Lane-Free Autonomous Driving. *Proc., 20th International Conference on Autonomous Agents and Multi-Agent Systems*, International Foundation for Autonomous Agents and Multiagent Systems, Online, May 3–7, 2021.
  30. Troullinos, D., G. Chalkiadakis, D. Manolis, I. Papamichail, and M. Papageorgiou. Lane-Free Microscopic Simulation for Connected and Automated Vehicles. *Proc., IEEE International Intelligent Transportation Systems Conference (ITSC)*, IEEE, New York, 2021, pp. 3292–3299.
  31. Rostami-Shahrbabaki, M., H. Zhang, M. Sekeran and K. Bogenberger. Increasing the Capacity of a Lane-Free

- Beltway for Connected and Automated Vehicles Using Potential Lines. In *102nd Annual Meeting Transportation Research Board*, (No. TRBAM-23-05268), Washington, D.C., 2023.
32. Reynolds, C. Flocks, Herds and Schools: A Distributed Behavioral Model. *Proc., 14th Annual Conference on Computer Graphics and Interactive Techniques*, Association for Computing Machinery, New York, 1987, pp. 25–34.
  33. Katz, Y., K. Tunström, C. Ioannou, C. Huepe, and I. Couzin. Inferring the Structure and Dynamics of Interactions in Schooling Fish. *Proceedings of the National Academy of Sciences of the United States of America*, Vol. 108, 2011, pp. 18720–18725.
  34. Hemelrijk, C., and H. Hildenbrandt. Schools of Fish and Flocks of Birds: Their Shape and Internal Structure by Self-Organization. *Interface Focus*, Vol. 2, 2012, pp. 726–737.
  35. Ibele, M., T. Mallouk, and A. Sen. Schooling Behavior of Light-Powered Autonomous Micromotors in Water. *Angewandte Chemie (International Ed. In English)*, Vol. 48, 2009, pp. 3308–3312.
  36. Desai, J., J. Ostrowski, and V. Kumar. Modeling and Control of Formations of Nonholonomic Mobile Robots. *IEEE Transactions on Robotics and Automation*, Vol. 17, 2001, pp. 905–908.
  37. Savkin, A. Coordinated Collective Motion of Groups of Autonomous Mobile Robots: Analysis of Vicsek’s Model. *IEEE Transactions on Automatic Control*, Vol. 49, 2004, pp. 981–983.
  38. Vásárhelyi, G., C. Virágh, G. Somorjai, T. Nepusz, A. Eiben, and T. Vicsek. Optimized Flocking of Autonomous Drones in Confined Environments. *Science Robotics*, Vol. 3, No. 20, 2018. <https://doi.org/10.1126/scirobotics.aat3536>.
  39. Russell Carpenter, J. Decentralized Control of Satellite Formations. *International Journal of Robust and Nonlinear Control*, Vol. 12, 2002, pp. 141–161.
  40. Olfati-Saber, R., J. Fax, and R. Murray. Consensus and Cooperation in Networked Multi-Agent Systems. *Proceedings of the IEEE*, Vol. 95, 2007, pp. 215–233.
  41. Olfati-Saber, R. Flocking for Multi-Agent Dynamic Systems: Algorithms and Theory. *IEEE Transactions on Automatic Control*, Vol. 51, 2006, pp. 401–420.
  42. Tang, C., and Y. Li. Consensus-Based Platoon Control for Non-Lane-Discipline Connected Autonomous Vehicles Considering Time Delays. *Proc., 37th Chinese Control Conference (CCC)*, IEEE, New York, 2018, pp. 7713–7718.
  43. Chuang, Y.-L., Y. R. Huang, M. R. D’Orsogna, and A. L. Bertozzi. Multi-Vehicle Flocking: Scalability of Cooperative Control Algorithms Using Pairwise Potentials. *Proc., IEEE International Conference on Robotics and Automation*, IEEE, New York, 2007, pp. 2292–2299.
  44. Wilson, R., *Introduction to Graph Theory*. Pearson Education India, New York, NY, 1979.
  45. Ricker, N. Wavelet Functions and Their Polynomials. *Geophysics*, Vol. 9, 1944, pp. 314–323.
  46. Malekzadeh, M., D. Manolis, I. Papamichail, and M. Papageorgiou. Empirical Investigation of Properties of Lane-Free Automated Vehicle Traffic. *Proc., IEEE International Intelligent Transportation Systems Conference (ITSC)*, IEEE, New York, 2022, pp. 2393–2400.